A R C H I V E S O F M E T A L L U R G Y A N D M A T E R I A L S
Volume 58 2013 Issue 2
DOI: 10.2478/amm-2013-0009

A. CZERWIŃSKI*, A. SKWAREK**, M. PŁUSKA*, J. RATAJCZAK*, K. WITEK**

WHISKER GROWTH IN TIN ALLOYS ON GLASS-EPOXY LAMINATE STUDIED BY SCANNING ION MICROSCOPY AND ENERGY-DISPERSIVE X-RAY SPECTROSCOPY

BADANIE WZROSTU WISKERÓW W STOPACH CYNY NA LAMINACIE SZKLANO-EPOKSYDOWYM Z UŻYCIEM SKANINGOWEJ MIKROSKOPII JONOWEJ I DYSPERSYJNEJ SPEKTROSKOPII RENTGENOWSKIEJ

Tin-rich solders are widely applied in the electronic industry in the majority of modern printed circuit boards (PCBs). Because the use of lead-tin solders has been banned in the European Union since 2006, the problem of the bridging of adjacent conductors due to tin whisker growth (limited before by the addition of Pb) has been reborn. In this study tin alloys soldered on glass-epoxy laminate (typically used for PCBs) are considered. Scanning ion microscopy with Focused Ion Beam (FIB) system and energy-dispersive X-ray spectroscopy (EDXS) were used to determine correlations between spatial non-uniformities of the glass-epoxy laminate, the distribution of intermetallic compounds and whisker growth.
Keywords: tin whiskers, tin-rich lead-free solders, intermetallic compounds (IMCs)

Bezołowiowe stopy lutownicze o wysokiej zawartości cyny są szeroko stosowane w przemyśle elektronicznym we współczesnych obwodach drukowanych (PCB). Stosowanie ołowiu w tych stopach jest od 2006 roku zakazane w Unii Europejskiej, co odnowiło problem wzrostu wiskerów cynowych poprzednio ograniczonego dodatkiem Pb. Wiskery zagrażają niezawodności układów elektronicznych, m.in. z powodu wprowadzanych zwarć. Praca dotyczy wzrostu wiskerów na powierzchni lutów naniesionych na najczęściej stosowany laminat szklano-epoksydowy. W oparciu o wyniki skaningowej mikroskopii jonowej (wykorzystującej zogniskowaną wiązkę jonów) i spektroskopii dyspersji energii promieniowania rentgenowskiego określono związek pomiędzy przestrzennymi niejednorodnościami laminatu szklano-epoksydowego, rozkładu wytrąceń międzymetalicznych i wzrostu wiskerów.

1. Introduction

Tin-rich solders are widely applied in the electronics industry, being used in manufacturing processes of the majority of modern printed circuit boards (PCBs). Tin whiskers are crystals growing from tin or tin alloy surface that are a threat to the reliability of electronic circuits because of short circuits (due to the bridging of adjacent conductors), increased electromagnetic radiation or device littering [1,2]. The phenomenon can occur in tin-rich solders, but the addition of lead to the tin alloy inhibits whisker growth. In the twentieth century, the most popular solder was Pb37Sn63 eutectics. However, since July 2006, and the Restriction of Hazardous Substances (RoHS) Directive adopted by the European Union, the amount of Pb in solders has been limited to 0.1 wt.%. The application of tin-rich lead-free solders in the PCB assembly process has reintroduced the problem of tin whisker growth which had been limited before by the addition of Pb. Whiskers are responsible for many system failures in the military, medical and telecommunication industries.

There is no single, commonly accepted model of whisker growth in the literature [2]. However, most theories involve the role of compressive stress [2-5], which may result from chemical, mechanical and thermal factors, with the whisker growth as a phenomenon of stress relief. The growth is affected by such factors as temperature, residual stress, mechanical force, the formation of intermetallic compounds (IMCs), broken oxide layer, electric field, etc. The higher the compressive stress, the greater the volume of Sn contained in whiskers [6].

In typical PCBs with a copper layer above a laminate substrate, the compressive stress generated as a result of volume expansion during the formation of IMCs (a Cu-Sn alloy formed at the Sn/Cu interface), is generally regarded as the driving force for Sn whisker growth. Whisker formation during thermal stress is also induced to a great extent by compressive stress resulting from the thermal expansion coefficient (CTE) mismatch of different layers. It has also been observed that when a tin-alloy layer is deposited on copper and there is compressive stress induced by IMCs created at the interface between tin and copper, the compressive stress near the surface is lower for thicker films, which therefore are more resistant for tin whisker formation [7,8]. Although full agreement has not yet been reached, it is suggested that when tin plating is

* INSTITUTE OF ELECTRON TECHNOLOGY, AL. LOTNIKOW 32/46, 02-668 WARSAW, POLAND
** INSTITUTE OF ELECTRON TECHNOLOGY, KRAKOW DIVISION, ZABLOCIE 39, 30-701 KRAKOW, POLAND

over 5 μm [9] (or 8 μm [10]) thick then the layer is more resistant to the whisker growth. Thicknesses below 0.5 μm and above 20 μm retard growth even more [9], although these very thin or thick plates may not be feasible in practice.

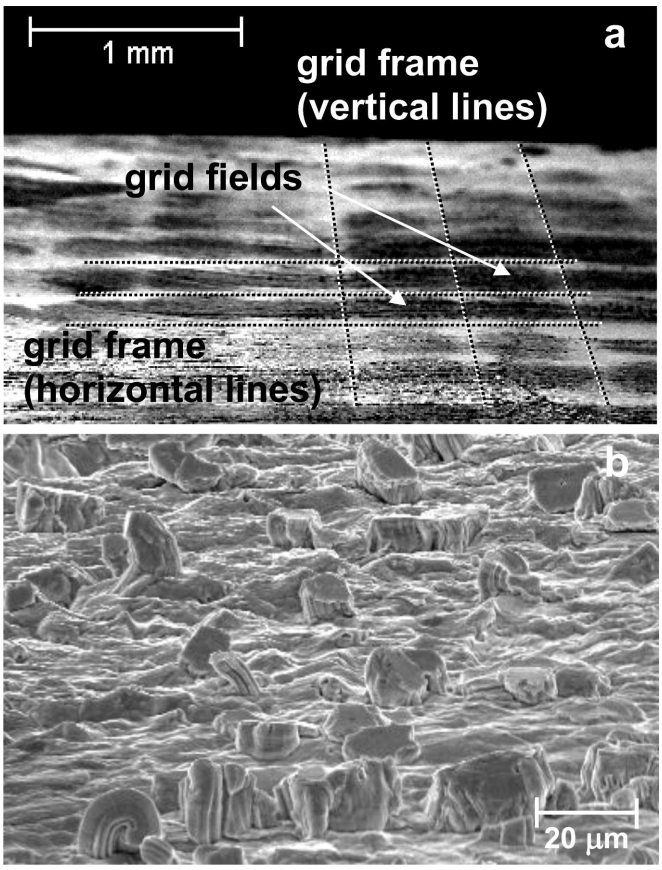

Fig. 1. (a) SEM image of an alloy surface soldered on glass-epoxy laminate (with a Cu layer) with a visible grid of rectangular grid-field regions (with hillocks and whiskers) and surrounding them grid-frame regions (i.e. flat areas practically without surface roughness). Image was taken after tilting the sample to attain better visibility of the grid. (b) Whiskers and hillocks visible within the region of grid field

The present paper concerns the whisker growth on the surface of tin-rich, lead-free alloys soldered on a Cu layer above a non-conductive glass-epoxy laminate (FR-4), i.e. with epoxy resin and woven fiberglass reinforcement, which is the most widely used PCB substrate material [11]. The glass-epoxy laminate is a mixture of two materials resin and glass fiber, with the resin filling the empty spaces between glass fibers. It was shown previously in [12] that the structure of the glass-epoxy laminate-surface has a fabric-like spatial non-uniformity caused by the regular structure of woven glass fibers and resin regions [12]. Precise analysis of the glass-epoxy surface (before the deposition of the solder) showed that in a general planar view, a grid is apparent. The same grid pattern was visible on the surface of a tin alloy soldered over a glass-epoxy laminate after standard reliability tests of temperature cycling conditions (Fig. 1). The structure of the laminate is responsible for forming the grid pattern visible on the solder surface. Local compressive stress in the solder layer due to large differences in the coefficient of thermal expansion (CTE) of the resin and glass fiber promotes whisker growth in the area of the alloy soldered on the Cu layer over the glass fiber (Fig. 1), i.e. in regions of grid fields of the visible grid pattern [12]. The coefficient of thermal expansion is much higher for the resin (e.g. about 63 ppm/°C), than for the glass fiber (about 5 ppm/°C) [11], while for tin and copper it is equal to 23 ppm/°C and 16.5 ppm/°C, respectively. This effect does not occur for an alloy soldered on Cu over e.g. a paper-phenol laminate. The lines of the grid frame correspond to the area of the solder placed over the resin while the grid fields between the grid frames correspond to the area of the solder placed over the glass fiber in a cross-section [12].

2. Experimental

The studied samples were PCB glass-epoxy laminate covered by a Cu foil (at least 17 μm thick) with a layer of tin or other, commercially available tin rich solder alloys: Sn100C (Sn99.3Cu0.7Ni), Sn99Cu1, Sn97Cu3, Sn99.5Ag3Cu0.5, Sn99.3Cu0.7AgNiGe, and Sn99Ag0.3Cu0.7NiGe. The alloys were applied by hand soldering with the application of a water flux. The soldering temperature was dependent on the alloy composition.

The samples were tested in a VÖTSCH chamber for 1500 shocks within a cyclic temperature range of -45°C to +85°C, with each cycle lasting 20 min and the transition time of the lift between hot and cold zones equal to 5 s. These conditions are recommended by NEMI (National Electronics Manufacturing Initiative) and JEDEC (Joint Electronic Device Engineering Council) as inducing whisker growth in most Sn and Sn-alloy layers [13].

The FEI Helios NanoLab 600 DualBeam Focused Ion Beam (FIB) system was applied to the milling (cross-sectioning) of samples with a precise gallium ion beam and also for scanning ion microscopy imaging (i.e. induced by the ion beam and detected by the secondary-electron detector) for the range of energies up to 30 keV. The cross sections were thoroughly cleaned in FIB to remove contaminations introduced during the FIB cross sectioning process [14, 15]. Energy-Dispersive X-ray Spectroscopy (EDXS) with a Philips XL30 scanning electron microscope (SEM) and EDAX spectrometer (with 130 eV spectral resolution) was used, with an energy range from 5 to 15 keV applied in the considered case.

3. Results and discussion

Scanning ion microscopy imaging and EDXS measurements were performed at various points on the mentioned grid to determine the correlations between the spatial non-uniformities of the structure of glass-epoxy laminate, of IMC distribution in the solder and of whisker growth after standard reliability tests. The grid on the solder is formed by grid fields (rectangular regions with hillocks and whiskers) surrounded by the grid frame (flat regions without surface roughness).

The measurements were first performed when the samples were observed in a planar view, with the sample surface placed perpendicular to the electron beam. Results obtained from grid fields (with hillocks and whiskers) showed a sig-

nificant Cu content, much higher than that from grid frames where this content was negligible.

Afterwards, FIB was used for milling samples with a gallium ion beam. These cross-sections were performed at several adjacent points spaced along a line from the grid frame to the grid field, with the aim of comparing neighboring points (instead of comparing random points in these two regions, because additional factors may be relevant in remote locations).

Images of cross-sectioned layers were taken by use of electron and ion microscopy. The scanning ion microscopy performed in FIB system, where detected secondary electrons are generated by the incident gallium ions, allowed for better image contrast than that observed in images obtained from standard secondary-electron (SE) or backscattered-electron (BSE) modes of SEM. Various tin alloy, copper and IMC grains look quite different in these FIB images (Figs. 2, 3), due to significantly different ion channeling inside various grains even in the case of the same material, e.g. tin alloy [16].

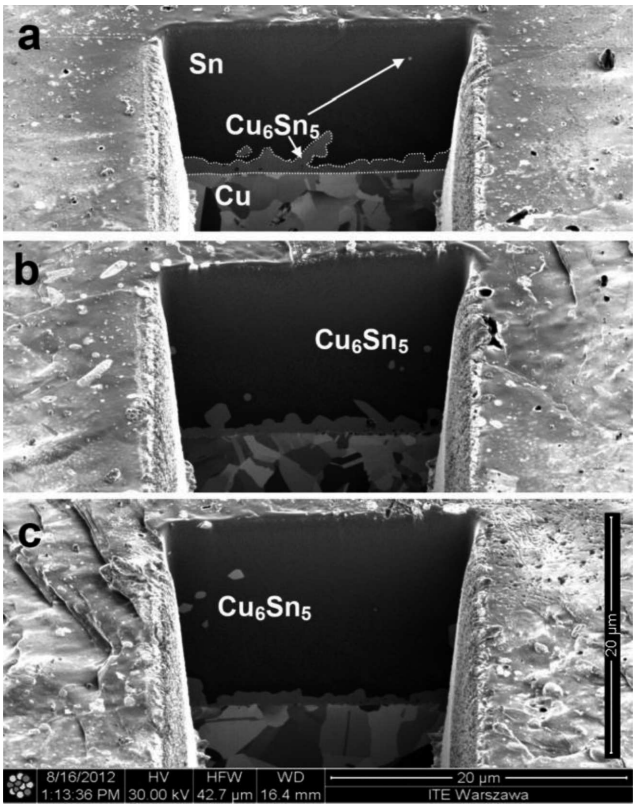

Fig. 2. Scanning ion microscopy image of cross sections milled by FIB in three consecutive adjacent places along a line from the grid-frame to the grid-field region: (a, b) in the grid-frame region, (c) at the boundary between the grid-frame and the grid-field regions. Going from the bottom to the top, the copper film, the interface IMC layer (with IMC protrusions extending upwards) and the solder layer (with small separate Cu_6Sn_5 precipitates inside) becoming thicker towards the grid-field region, are visible in these cross sections. Small dotted lines drawn along boundaries of IMC layer (at the alloy/Cu interface) enhance its visibility in the figure (a). Due to tilting of the sample the vertical marker is different from the horizontal one

Cross-section images show three metallic layers above the laminate: a Cu layer at the bottom, a tin-alloy layer on the top and a thin IMC layer between them. The studies revealed a distinct difference between distinguished regions of grid frames and grid fields with respect to the quantity, size and location of IMC precipitates within the solder layer (Figs. 2 and 3). Although in the region of grid frames even long Cu_6Sn_5 protrusions extended into the solder layer from the IMC layer (i.e. situated at the interface between the layers of tin-alloy and copper), but only small IMC precipitates (with a sub-micrometer diameter) were observable inside the solder layer, i.e. without a direct contact with the IMC layer (Figs. 2a,b).

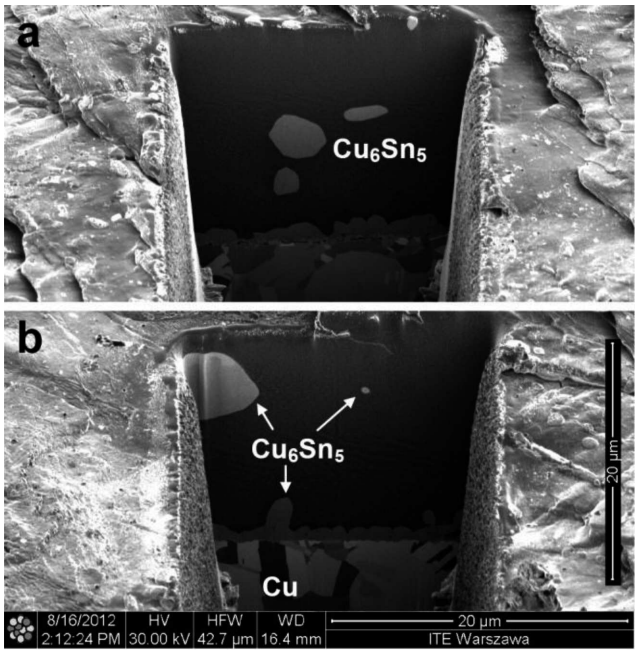

Fig. 3. Scanning ion microscopy image of cross sections milled by FIB in the grid field region in the two consecutive adjacent places along a line from the grid-frame to the grid-field region (situated next to the three places shown in Fig. 2). Going from the bottom to the top the copper film, the interface IMC layer and the solder layer (with large separate Cu_6Sn_5 precipitates inside) are visible in these cross sections. Due to tilting of the sample the vertical marker is different from the horizontal one

In contrast, in the region of grid fields much bigger IMC precipitates (with diameters even in the range 5-8 μm) were observed inside the solder layer, without a direct contact with the IMC layer and close to the solder top surface (Figs. 3a,b). In many cases densely distributed round-shaped Cu_6Sn_5 precipitates with diameters from one to several micrometers even reached the top surface of the tin alloy and these were observable at close distances from each other (Fig. 4). The occurrence of IMC precipitates on solder surfaces has been observed previously [17].

Numerous previous observations have shown and discussed IMC protrusions extending from the IMC layer into the solder layer as well as have shown IMC precipitates located within the solder layer and positioned along grain boundaries [18, 19]. However, in our investigations (as well as observations in some other studies [20]) Cu_6Sn_5 precipitates were found not only along grain boundaries but also inside the solder grains, i.e. without a visible contact with grain boundaries (Figs. 2, 3 and 5). Separate Cu_6Sn_5 precipitates were also observed even inside some whisker crystals (Fig. 5), confirming that during their upward migration IMCs can penetrate

into various grains. It can also be seen in this figure that the density of IMC precipitates in the solder increases closer to the whisker.

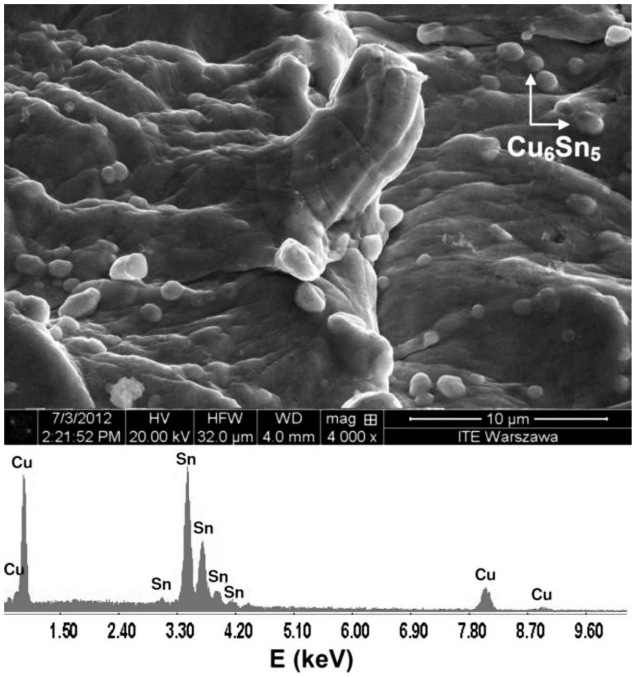

Fig. 4. SEM image of a single whisker. Densely distributed round-shaped Cu_6Sn_5 precipitates at the top surface of the tin alloy at the grid field are visible close to the whisker apparent in the center of the image. EDXS spectrum (obtained at electron energy 15 keV) of an example precipitate is shown below

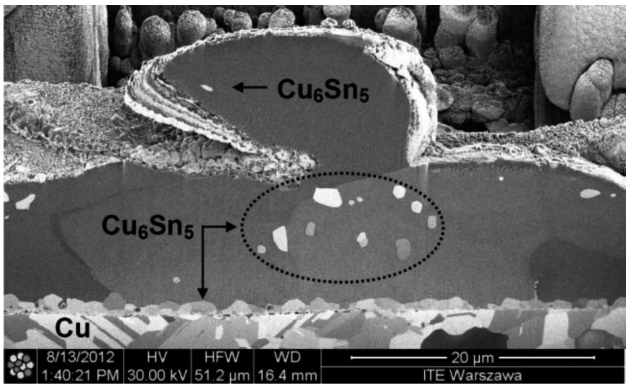

Fig. 5. Scanning ion microscopy image of a cross section with a whisker grown in the grid-frame region. An increased density of Cu_6Sn_5 precipitates in the tin alloy solder close to the whisker base and a small separate Cu_6Sn_5 precipitate inside the whisker are seen

Generally, during the soldering operation, material from the metal sublayer dissolves and mixes with the solder, allowing the formation of IMCs. In alloys consisting of Sn and Cu, two different phases of IMCs may be present: Cu_6Sn_5 and Cu_3Sn. Especially the formation of a Cu_6Sn_5 phase (because of its large volume expansion in comparison with the pure tin) is a strong factor promoting whisker growth in the neighboring alloy [3]. Our EDXS measurements revealed a content of about 39 wt.% Cu in the IMC layer at the interface between copper and tin alloy layers, i.e. measurably equal to the Cu content in the Cu_6Sn_5 layer. The same content of about 39 wt.% Cu was found for all measured IMC precipitates observed within the tin-alloy layer, confirming that they also constituted a Cu_6Sn_5 phase. In contrast, the content of Cu in another possible Cu-Sn IMC phase (i.e. Cu_3Sn) would be equal to above 60 wt.% Cu, much higher than revealed in our measurements.

In contrast, no distinguishable difference in the shape of the interface IMC layer was observed between the two regions (of the grid frame and of grid fields) (Figs. 2 and 3). This means that the spatial non-uniformity caused by the regular structure of glass fibers and resin regions in the top layer of a glass-epoxy laminate also promotes spatial non-uniformity of the IMC-precipitate distribution within the solder layer, often close to its top surface. This effect seems to constitute an additional factor for the apparent non-uniformity of whisker growth.

Thick solder layers (significantly above 10 μm) were applied in samples to ensure their resistance to whisker growth. Cross sections performed in regions adjacent to grid frames and grid fields show that the thickness of tin alloy in the frame regions is significantly lower than in the field regions, e.g. equals about 13 μm at the grid frame (Fig. 2a) while about 18 μm in the adjacent regions of grid fields (Fig. 3a,b).

The calculation of alloy thickness takes into account that the studied samples were tilted during observations in the microscope chamber. Thus markers shown in Figs. 2, 3 and 5 represent horizontal dimensions, while the vertical dimensions are underestimated and therefore their multiplication by the tilt angle secant is required(i.e. by 1.24, because the tilt angle equals 36° there).

Whisker growth depends on many factors with an impact of one factor being distinguishable only when other important factors are fixed. Although a thinner (if not very thin) solder is considered to be more prone to whisker growth [7-10], the mentioned additional factors related to the compressive stress have forced an absence of whiskers in grid frame regions (with thinner solder), and their presence in regions of grid fields (with thicker solder).

Much higher thermal expansion coefficient of the resin than of the glass fiber causes the resin to expand and shrink more than the glass fiber during tests performed with a cyclic temperature range of -45°C to +85°C. A nonuniform expansion of the top area of the glass-epoxy laminate occurs in its longisection, as well as in its cross-section. It may be expected that alongside differences in compressive stress in adjacent regions, the layers in various regions will be differently affected mechanically, shifted and pushed up during temperature cycles. The observed non-uniform spatial distribution of IMC precipitates seems to occur due to differences in mechanical interactions and compressive stress in various regions, while the presence of IMCs is a driving force for whisker growth. Therefore, it may be expected that CTE differences in various regions of PCBs with tin-alloy on glass-epoxy laminate facilitate spatially non-uniform whisker growth in two ways, directly by the implemented compressive stress and indirectly by the generation of non-uniform IMC distribution.

4. Summary

Whisker growth on the surface of tin alloys soldered above a glass-epoxy laminate was studied, i.e. for the most widely used PCB substrate material. The structure of the glass-epoxy laminate surface has a spatial non-uniformity caused by the regular structure of glass fibers and resin regions in the top layer of the laminate. Therefore, the local compressive stress in the solder layer due to differences in the thermal expansion of the resin and glass fiber promotes whisker growth in the area of the alloy soldered on the Cu layer over the glass fiber.

Scanning ion microscopy using the FIB system and EDXS performed after standard reliability tests determined a strong correlation between the structure of glass-epoxy laminate, the spatial distribution of IMCs and whisker growth. In the region of grid frames only small IMC precipitates were observable inside the solder layer (i.e. without a direct contact with the IMC layer situated at the interface between the tin-alloy and Cu layers). In contrast, in the region of grid fields much bigger IMC precipitates were observed inside the solder layer, without a contact with the IMC layer and close to the solder top surface. Densely distributed round-shaped Cu_6Sn_5 precipitates with diameters from one to several micrometers also reached the top surface of solder in many places.

It can be concluded that CTE differences of various PCB regions with tin-alloys on glass-epoxy laminate facilitate spatially non-uniform whisker growth directly by the non-uniform compressive stress and indirectly by the generation of a non-uniform spatial distribution of IMCs.

Acknowledgements

The work has been partially supported by the National Science Centre (project no N N515 503940).

REFERENCES

[1] D. Pinsky, M. Osterman, S. Ganesan, IEEE Transactions on Components and Packaging Technologies **27**, 427 (2004).

[2] G.T. Galyon, IEEE Transactions on Electronics Packaging Manufacturing **28**, 94 (2005).

[3] G.T. Galyon, L. Palmer, IEEE Transactions on Electronics Packaging Manufacturing **28**, 17 (2005).

[4] C. Xu, Y. Zhang, C. Fan, J.A. Abys, IEEE Transactions on Electronics Packaging Manufacturing **28**, 31 (2005).

[5] J. Smetana, IEEE Transactions on Electronics Packaging Manufacturing **30**, 11 (2007).

[6] J. Cheng, S. Chen, P.T. Vianco, J.C.M. Li, Journal of Applied Physics **107**, 074902 (2010).

[7] B.D. Dunn, A laboratory study of tin whisker growth, ISSN 0379 4067, European Space Agency (1987), http://nepp.nasa.gov/whisker/reference/tech_papers/dunn1987-a-lab-study-of-tin-whisker-growth.pdf

[8] J. Cheng, F. Yang, P.T. Vianco, B. Zhang, J.C.M. Li, Journal of Electronic Materials **40**, 2069 (2011).

[9] X.C. Tong, Advanced Materials for Thermal Management of Electronic Packaging (Springer Series in Advanced Microelectronics) Schaumburg 2011.

[10] R. Schetty, Circuit World **27**, 17 (2001).

[11] R. Sanapala, Characterization of FR-4 Printed Circuit Board Laminates Before and After Exposure to Lead-free Soldering Conditions, ProQuest LLC, Ann Arbor, 2008.

[12] A. Skwarek, M. Pluska, A. Czerwinski, K. Witek, Materials Science and Engineering **B177**, 1286 (2012).

[13] N. Vo, M. Kwoka, P. Bush, IEEE Transactions on Electronics Packaging Manufacturing **28**, 3 (2005).

[14] J. Orloff, M. Utlaut, L. Swanson, High Resolution Focused Ion Beam: FIB and Its Applications, Kluwer Academic/Plenum Press, New York 2003.

[15] L.A. Giannuzzi, F.A. Stevie, Introduction to Focused Ion Beams: Instrumentation, Theory, Techniques and Practice, Springer, New York 2005.

[16] S.W. Liang, C. Chen, J.K. Han, L. Xu, K.N. Tu, Y.-S. Lai, Journal of Applied Physics **107**, 093715 (2010).

[17] S. Choi, K.N. Subramanian, J.P. Lucas, T.R. Bieler, T.R., Journal of Electronic Materials **29**, 1249 (2000).

[18] G.T.T. Sheng, C.F. Hu, W.J. Choi, K.N. Tu, Y.Y. Bong, L. Nguyen, Journal of Applied Physics **92**, 64 (2002).

[19] K.N. Tu, J.C.M. Li, Materials Science and Engineering A **409**, 131 (2005).

[20] C.-F. Yu, C.-M. Chan, K.-C. Hsieh, Microelectronics Reliability **50**, 1146 (2010).

Received: 20 January 2013.